Thin Film Transistors Based on Alkylphenyl Quaterthiophenes: Structure and Electrical Transport Properties

Sandra E. Fritz,[†] Siddharth Mohapatra,[†] Brian T. Holmes,[†] Amelia M. Anderson,[†] Cathal F. Prendergast,[†] C. Daniel Frisbie,*[,†] Michael D. Ward,*[,†] and Michael F. Toney[‡]

Department of Chemical Engineering and Materials Science, University of Minnesota, Minneapolis, Minnesota 55455, and Stanford Synchrotron Radiation Laboratory, Stanford Linear Accelerator Center, 2575 Sand Hill Road, M/S 69, Menlo Park, California 94025

Received November 28, 2006. Revised Manuscript Received January 16, 2007

Thin films based on the akylphenyl-substituted quaterthiophenes 5,5‴-bis(4-methylphenyl)-2,2′:5′,2″:5″,2‴-quaterthiophene (**1**), 5,5‴-bis(4-*n*-propylphenyl)-2,2′:5′,2″:5″,2‴-quaterthiophene (**2**), and 5,5‴-bis(4-hexylphenyl)-2,2′:5′,2″:5″,2‴-quaterthiophene (**3**) were grown by vacuum deposition on thermally grown SiO_2 substrates and characterized in a thin film transistor (TFT) configuration. Atomic force microscopy and specular ($\theta-2\theta$) X-ray diffraction (XRD) revealed films with small, crystalline grains, in which the oligothiophenes were oriented "end-on" with respect to the SiO_2 substrate. Interplanar spacing increased (**1** = 28.0 Å, **2** = 29.5 Å, **3** = 37.7 Å), consistent with increasing alkyl tail length. Grazing incidence X-ray diffraction (GIXD) of the films (ca. 350 Å thick) revealed nearly equivalent in-plane unit-cell areas (**1** = 44.1 Å^2, **2** = 44.4 Å^2, **3** = 43.8 Å^2). The films functioned as *p*-channel semiconductors in a TFT configuration, exhibiting nearly equivalent hole mobilities ($\mu \approx 0.05 \pm 0.01$, 0.04 ± 0.01, 0.06 ± 0.01 cm^2/Vs for **1**, **2**, and **3**, respectively). Variable-temperature measurements demonstrated that the activation energy of the mobility for thin films of **3** was ∼55 meV. The increasing alkyl chain length does not appear to improve molecular ordering; however, the addition of a phenyl end-substituent appears to greatly improve the on-to-off ratio in TFTs.

Introduction

Oligothiophenes, such as sexithiophene and its modified forms, have emerged as attractive candidates for hole-transport materials in organic thin film transistors (TFTs) because of their stability and the ease with which their electronic properties and solubility characteristics can be adjusted through the introduction of chemical substituents.[1−11] The introduction of "end-cap" substituents at the 2-position can provide stability against oxidation and polymerization while minimizing steric interactions that can prohibit coplanarity of the thiophene rings, as observed for oligothiophenes with alkyl substituents on the backbone.[12,13] Properly designed end-cap substituents may improve crystallinity, encourage layer growth conducive to carrier transport in TFTs, and promote dense intermolecular packing in two-dimensional layers, yielding gains in intrinsic conductivity.[14] For example, the superior hole mobility exhibited by oligothiophenes with alkyl substituents at the 2-position[15−21] has been attributed to improved crystallinity and layer growth, the latter favoring hole transport in the direction parallel to the film.[22] Phenylene substituents introduced at the 2-position[23] or within the oligothiophene backbone[24] can

* Corresponding author. E-mail: wardx004@umn.edu (M.D.W.); frisbie@cems.umn.edu (C.D.F.).
[†] University of Minnesota.
[‡] Stanford Linear Accelerator Center.

(1) *Handbook of Organic Conductive Molecules and Polymers*; Nalwa, H. S., Ed.; John Wiley & Sons: New York, 1997; Vol. 1−4.
(2) Facchetti, A.; Yoon, M. H.; Stern, C. L.; Katz, H. E.; Marks, T. J. *Angew. Chem., Int. Ed.* **2003**, *42*, 3900.
(3) Wei, Y.; Yang, Y.; Yeh, J. *Chem. Mater.* **1996**, *8*, 2659.
(4) Pappenfus, T. M.; Chesterfield, R. J.; Frisbie, C. D.; Mann, K. R.; Casado, J.; Raff, J. D.; Miller, L. L. *J. Am. Chem. Soc.* **2002**, *124*, 4184.
(5) Bader, M. M.; Custelcean, R.; Ward, M. D. *Chem. Mater.* **2003**, *15*, 616.
(6) Garnier, F.; Yassar, A.; Hajlaoui, R.; Horowitz, G.; Deloffre, F.; Servet, B.; Ries, S.; Alnot, P. *J. Am. Chem. Soc.* **1993**, *115*, 8716.
(7) Mushrush, M.; Fachetti, A.; Lefenfield, M.; Katz, H. E.; Marks, T. J. *J. Am. Chem. Soc.* **2003**, *125*, 31.
(8) Leclère, Ph.; Surin, M.; Viville, P.; Lazzaroni, R.; Kilbinger, A. F. M.; Henze, O.; Feast, W. J.; Cavallini, M.; Biscarini, F.; Schenning, A. P. H. J.; Meijer, E. W. *Chem. Mater.* **2004**, *16*, 4452.
(9) Dell'Aquila, A.; Mastrorilli, P.; Nobile, C. F.; Romanazzi, G.; Suranna, G. P.; Torsi, L.; Tanese, M. C.; Acierno, D.; Amendola, E.; Morales, P. *J. Mater. Chem.* **2006**, *16*, 1183.
(10) Murphy, A. R.; Chang, P. C.; VanDyke, P.; Liu, J.; Fréchet, J. M. J.; Subramanian, V.; DeLongchamp, D. M.; Sambasivan, S.; Fischer, D. A.; Lin, E. K. *Chem. Mater.* **2005**, *17*, 6033.
(11) Chang, P. C.; Lee, J.; Huang, D.; Subramanian, V.; Murphy, A. R.; Fréchet, J. M. J. *Chem. Mater.* **2004**, *16*, 4783.
(12) Barbarella, G.; Zambianchi, M.; Antolini, L.; Ostoja, P.; Maccagnani, P.; Bongini, A.; Marseglia, E. A.; Tedesco, E.; Gigli, G.; Cingolani, R. *J. Am. Chem. Soc.* **1999**, *121*, 8920.
(13) Luzny, W. *Acta Crystallogr., Sect. B* **1995**, *51*, 255.
(14) Barclay, T. M.; Cordes, A. W.; Mackinnon, C. D.; Oakley, R. T.; Reed, R. W. *Chem. Mater.* **1997**, *9*, 981.
(15) Garnier, F.; Yassar, A.; Hajlauoi, R.; Horowitz, G.; Deloffre, F.; Servet, B.; Ries, S.; Alnot, P. *J. Am. Chem. Soc.* **1993**, *115*, 8716.
(16) Katz, H. E.; Dodabalapur, A.; Torsi, L.; Elder, D. *Chem. Mater.* **1995**, *7*, 2238.
(17) Ackermann, J.; Videlot, C.; Raynal, P.; Kassmi, A. El; Dumas, P. *Appl. Surf. Sci.* **2003**, *212*, 26.
(18) Halik, M.; Klauk, H.; Zschieschang, U.; Schmid, G.; Ponomarenko, S.; Kirchmeyer, S.; Weber, W. *Adv. Mater.* **2003**, *15*, 917.
(19) Deman, A.-L.; Tardy, J.; Nicolas, Y.; Blanchard, P.; Roncali, J. *Synth. Met.* **2004**, *146*, 365.
(20) Ackermann, J.; Videlot, C.; Dumas, P.; Kassmi, A. El; Guglielmetti, R.; Safarov, V. *Org. Electron.* **2004**, *5*, 213.
(21) Facchetti, A.; Mushrush, M.; Yoon, M.-H.; Hutchison, G. R.; Ratner, M. A.; Marks, T. J. *J. Am. Chem. Soc.* **2004**, *126*, 13859.
(22) Horowitz, G. *Adv. Mater.* **1998**, *10*, 365.

10.1021/cm062831v CCC: $37.00
Published on Web 02/22/2007

reduce TFT "off" currents,[25,26] a property that has been attributed to the lowering of the highest occupied molecular orbital (HOMO) and, consequently, a reduced propensity for doping upon exposure to oxygen.

The elucidation of the factors most critical to TFT performance requires systematic and comprehensive investigations of the relationship between molecular structure, thin film morphology, crystal orientation, molecular packing density, and transport properties. Recently, our laboratory examined the structure and transport properties of thin films based on a series of molecules, tolyl-nT-tolyl (molecules **1**, **4**, and **5**), in which the length of the oligothiophene core ($n = 3-5$) was adjusted systematically but the end-caps were unchanged.[27] Herein, we describe a converse approach in which the oligothiophene core is maintained constant ($n = 4$) but the alkylphenyl substituents are changed (R = methyl, propyl, and hexyl; compounds **1**, **2**, and **3**). Although TFTs based on vacuum- and solution-deposited films of **3** have been reported,[7] the studies presented here represent a more comprehensive examination aimed at understanding the relationship of film morphology, crystal structure, and trap states to transport. Thin films of these compounds exhibit *p*-channel behavior with mobilities comparable to those reported previously for **3**[7] and significantly improved on-to-off ratios in all three compounds that are comparable to values observed in films of pentacene. Atomic force microscopy (AFM) and specular ($\theta-2\theta$) X-ray diffraction (XRD) reveal that the films are crystalline and form domains with low mosaicity. Furthermore, grazing incidence X-ray diffraction (GIXD) reveals nearly identical in-plane unit-cell areas for compounds **1**−**3**, in agreement with the equivalent mobilities.

Experimental Section

Materials Synthesis and General Procedures. All synthetic procedures were performed under an inert nitrogen atmosphere with oven-dried glassware. Toluene and tetrahydrofuran were distilled (under nitrogen) from Na/benzophenone, and *N*,*N*′-dimethylformamide was vacuum distilled from 3 Å molecular sieves. All reagents and catalysts were purchased from Aldrich, Acros, and Alfa Aesar and used as received. Compounds 5,5′-bis(trimethylstannyl)-2,2′-dithiophene and 5,5‴-bis(4-methylphenyl)-2,2′:5′,2″:5″,2‴-quaterthiophene (**1**) were synthesized according to published procedures.[1,27] ^{1}H NMR spectra were recorded on a Varian VXR-300 MHz instrument. Chemical shifts are reported in parts per million (ppm) and referenced to the residual dichloromethane peak at 5.32 ppm.

Preparation of 2-Bromo-5-(4-*n*-propylphenyl)thiophene. A DMF (15 mL) mixture of 1-bromo-4-*n*-propylbenzene (0.54 mL, 3.48 mmol), 2-(tri-*n*-butylstannyl)thiophene (1.0 mL, 3.17 mmol), and tetrakis(triphenylphosphine)palladium(0) (0.179 g, 0.15 mmol) was heated at 90 °C overnight under nitrogen. After the reaction was cooled to room temperature, ammonium chloride (50 mL) and hexane (50 mL) were added, the organic layer was separated, and the aqueous layer was extracted with hexane (2 × 50 mL). The organic layers were combined, washed with water (2 × 50 mL), dried with $MgSO_4$, filtered, and concentrated in vacuo to yield a yellow oil. After purification by column chromatography on silica gel (hexane), 2-(4-*n*-propylphenyl)thiophene was obtained as a clear oil (0.57 g, 90.0%). ^{1}H NMR (300 MHz, CD_2Cl_2): δ 7.52−7.57 (m, 2H), 7.18−7.30 (m, 4H), 7.05−7.10 (m, 1H), 2.61 (t, 2H, J = 7.2 Hz), 1.57−1.77 (m, 2H), 0.91−1.03 (m, 3H).

Dry DMF (12 mL) was added to 2-(4-*n*-propylphenyl)thiophene (0.573 g, 2.83 mmol), and the mixture was cooled to −5 °C. *N*-Bromosuccinimide (0.550 g, 3.12 mmol) was then added slowly to the chilled solution. After the solution was allowed to stand under nitrogen for 3 h, ice water (25 mL) was added to force precipitation of the product, which was filtered and washed with water. The resulting solid was dissolved in dichloromethane,; the solution was dried over $MgSO_4$, filtered, and concentrated in vacuo to yield a greasy yellow solid of the product 2-bromo-5-(4-*n*-propylphenyl)-thiophene (0.631 g, 78.1%). ^{1}H NMR (300 MHz, CD_2Cl_2): δ 7.43 (d, 2H, J = 8.2 Hz), 7.18 (d, 2H, J = 8.4 Hz), 7.01 (s, 2H), 2.56 (t, 2H, J = 8.2 Hz), 1.56−1.75 (m, 2H), 0.96 (t, 3H, J = 5.8 Hz). HREIMS: calcd for $C_{13}H_{13}BrS$ [M+], 279.9921; found, 279.9901. Anal. Calcd for $C_{13}H_{13}BrS$: C, 55.52; H, 4.66. Found: C, 55.55, H, 4.59.

Preparation of 5,5‴-Bis(4-*n*-propylphenyl)-2,2′:5′,2″:5″,2‴-quaterthiophene (2). A toluene solution (6 mL) of 2-bromo-5-(4-*n*-hexylphenyl)thiophene (0.230 g, 0.711 mmol), 5,5′-bis(trimethylstannyl)-2,2′-dithiophene (0.160 g, 0.323 mmol), and tetrakis(triphenylphosphine)palladium(0) (0.019 g, 0.036 mmol) was heated at 90 °C overnight under nitrogen. The resulting precipitate was collected, washed several times with methanol and hexanes, and dried in vacuo to yield a crude product (0.140 g, 67.0%). The crude product was recrystallized from 1,1,2-trichloroethane/toluene to yield an orange solid (56.8%). ^{1}H NMR (300 MHz, CD2Cl2): δ 7.53 (d, 4H, J = 7.7 Hz), 7.08−7.23(m, 12H), 2.62 (t, 4H, J = 7.7 Hz), 1.65−1.71 (m, 4H), 1.34−1.43 (m, 12H), 0.90 (t, 6H, J = 6.1 Hz). HREIMS: calcd for C40H42S4 [M+], 651.2169; found, 651.2161. Anal. Calcd for $C_{40}H_{42}S_4$: C, 73.80; H, 6.50. Found: C, 73.90; H, 6.44.

Preparation of 2-Bromo-5-(4-*n*-hexylphenyl)thiophene. A DMF (15 mL) mixture of 1-bromo-4-n-hexylbenzene (0.50 mL, 2.45 mmol), 2-(tri-n-butylstannyl)thiophene (0.78 mL, 2.45 mmol), and tetrakis(triphenylphosphine)palladium(0) (0.142 g, 0.123 mmol) was heated at 90 °C overnight under nitrogen. After the reaction was cooled to room temperature, ammonium chloride (50 mL) and hexane (50 mL) were added, the organic layer was separated, and the aqueous layer was extracted with hexane (2 × 50 mL). The organic layers were combined, washed with water (2 × 50 mL), dried with $MgSO_4$, filtered, and concentrated in vacuo to yield an orange oil. After purification by column chromatography on silica gel (hexane), 2-(4-*n*-hexylphenyl)thiophene was obtained as a clear oil (0.52 g, 87.0%). ^{1}H NMR (300 MHz, CD_2Cl_2): δ 7.49−7.53 (m, 2H), 7.16−7.27 (m, 4H), 7.03−7.08 (m, 1H), 2.60 (t, 2H, J = 7.9 Hz), 1.57−1.64 (m, 2H), 1.28−1.36 (m, 6H), 0.91 (t, 3H, J = 7.0 Hz).

Dry DMF (10 mL) was added to 2-(4-*n*-hexylphenyl)thiophene (0.521 g, 2.13 mmol), and the mixture was cooled to −5 °C. *N*-Bromosuccinimide (0.416 g, 2.34 mmol) was then added slowly to the chilled solution. After the solution was allowed to stand under nitrogen for 3 h, ice water (20 mL) was added to force precipitation of the product, which was filtered and washed with water. The resulting solid was dissolved in dichloromethane, and the solution

(23) Hotta, S.; Ichino, Y.; Yoshida, Y.; Yoshida, M. *Synth. Met.* **2001**, *121*, 1353.
(24) Hotta, S.; Ichino, Y.; Yoshida, Y.; Yoshida, M. *J. Phys. Chem. B* **2000**, *104*, 10316.
(25) Hong, X.-M.; Katz, H. E.; Lovinger, A. J.; Wang, B.-C.; Raghavachari, K. *Chem. Mater.* **2001**, *13*, 4686.
(26) Ponomarenko, S. A.; Kirchmeyer, S.; Elschner, A.; Alpatova, N. M.; Halik, M.; Klauk, H.; Zschieschang, U.; Schmid, G. *Chem. Mater.* **2006**, *18*, 579.
(27) Mohapatra, S.; Holmes, B. T.; Newman, C. R.; Prendergast, C. F.; Frisbie, C. D.; Ward, M. D. *Adv. Funct. Mater.* **2004**, *14*, 605.

was dried over $MgSO_4$, filtered, and concentrated in vacuo to yield a greasy yellow solid of the product 2-bromo-5-(4-*n*-hexylphenyl)-thiophene (0.590 g, 86.1%). ^{1}H NMR (300 MHz, CD2Cl2): δ 7.46 (d, 2H, J = 8.2 Hz), 7.21 (d, 2H, J = 8.3 Hz), 7.05 (s, 2H), 2.62 (t, 2H, J = 7.4 Hz), 1.66−1.73 (m, 2H), 1.22−1.34 (m, 6H), 0.94 (t, 3H, J = 6.8 Hz). HREIMS: calcd for C16H19BrS [M+], 322.0391; found, 322.0368. Anal. Calcd for C16H9BrS: C, 59.44, H, 5.92. Found: C, 59.34, H, 6.01.

Preparation of 5,5‴-Bis(4-*n*-hexylphenyl)-2,2′:5′,2″:5″,2‴-quaterthiophene (3). A toluene solution (6 mL) of 2-bromo-5-(4-n-hexylphenyl)thiophene (0.230 g, 0.711 mmol), 5,5′-bis(trimethylstannyl)-2,2′-dithiophene (0.160 g, 0.323 mmol), and tetrakis(triphenylphosphine)palladium(0) (0.019 g, 0.036 mmol) was heated at 90 °C overnight under nitrogen. The resulting precipitate was collected, washed several times with methanol and hexanes, and dried in vacuo to yield a crude product (0.140 g, 67.0%). The crude product was recrystallized from 1,1,2-trichloroethane/toluene to yield an orange solid (56.8%). ^{1}H NMR (300 MHz, CD2Cl2): δ 7.53 (d, 4H, J = 7.7 Hz), 7.08−7.23 (m, 12H), 2.62 (t, 4H, J = 7.7 Hz), 1.65−1.71 (m, 4H), 1.34−1.43 (m, 12H),0.90 (t, 6H, J = 6.1 Hz). HREIMS: calcd for $C_{40}H_{42}S_4$ [M+], 651.2169; found, 651.2161. Anal. Calcd for $C_{40}H_{42}S_4$: C, 73.80; H, 6.50. Found: C, 73.90; H, 6.44.

Structural, Thermal, and Electrical Characterization. Powder X-ray diffraction of thin films and bulk powders were acquired with a PANalytical X'Pert Pro (Almelo, The Netherlands) high-resolution X-ray diffractometer with Cu Kα_1 (λ = 1.5418 Å) maintained by the Characterization Facility at the University of Minnesota. Tapping mode atomic force microscope (AFM) images were recorded in air using a Digital Instruments Dimension AFM. Grazing Incidence X-ray Diffraction (GIXD) experiments were performed at the Stanford Synchrotron Radiation Laboratory (SSRL), beam line 7-2, at a wavelength of 1.549 Å and incidence angles of 0.2−0.24°. Thermal gravimetric/differential thermal analysis (TG/DTA) was performed using a Perkin-Elmer (Wellesley, MA) Pyris Diamond TG/DTA 6300. The temperature range was 25−400 °C with a ramp of 5 °C/min.

Thin Films of **1**−**3** were grown by vacuum sublimation at 1 × 10^{-7} Torr at a rate of 0.02−0.06 Å/s, on a 3 kÅ thick thermally grown SiO_2 on <100>-oriented single-crystal silicon substrates. The optimized substrate temperature, as deduced from the size and quality of the crystalline domains, was 50−95 °C. Gold top contacts were deposited by shadow masking. The TFT geometry used had a channel length of 200 μm and a width of 2000 μm.

Conductivity measurements were performed in the dark using a Desert Cryogenics probe station with a base pressure of 5 × 10^{-7} Torr (Desert Cryogenics, Phoenix, AZ). Temperature was controlled via a Lakeshore L-331 (Westerville, OH) controller between 80 and 295 K. Source and drain voltages were applied with a Keithley 236 and Keithley 237 source measure unit, respectively (Keithley, Cleveland, OH). Gate voltages were applied with a Keithley 6517A electrometer. Channel voltages were sensed with a pair of Keithley 6517A electrometers. Source and drain currents were independently monitored by the 236 and 237, respectively, to evaluate potential leaks in the devices. All four units shared a common ground with an input impedance of 1 × 10^{14} Ω.

Results and Discussion

Film Morphology and Structural Characterization. The homologous series of compounds 5,5‴-bis(4-methylphenyl)-2,2′:5′,2″:5″,2‴-quaterthiophene (**1**), 5,5‴-bis(4-propylphenyl)-2,2′:5′,2″:5″,2‴-quaterthiophene (**2**), and 5,5‴-bis(4-hexylphenyl)-2,2′:5′,2″:5″,2‴-quaterthiophene (**3**) exhibited

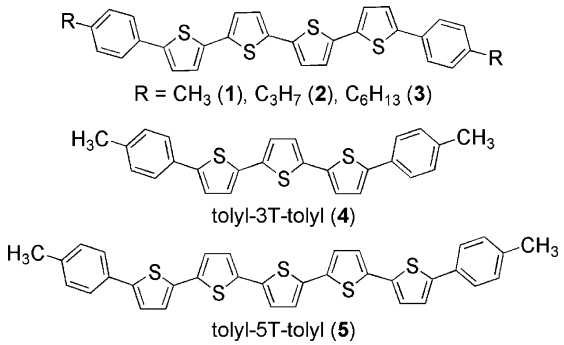

Figure 1. Chemical structures of alkylphenyl-oligothiophenes.

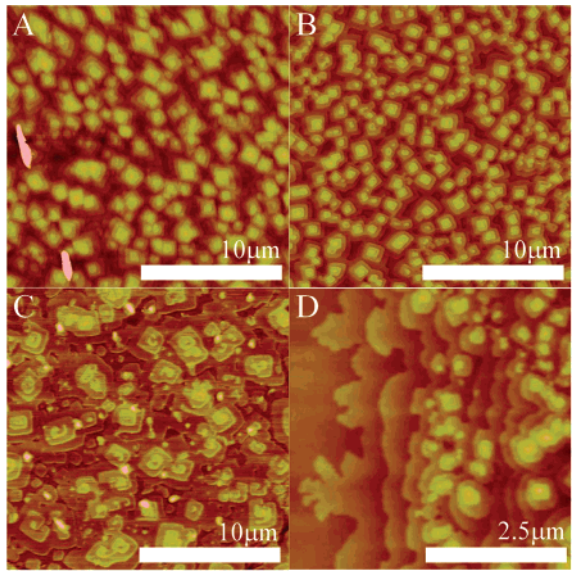

Figure 2. Topographic AFM images of (A) **1**, (B) **2**, and (C) **3** film morphology and (D) edge of a film of **2**. Substrate temperatures during depositions were 75 °C for **1** and **2** and 95 °C for **3**.

quasi-reversible one-electron oxidations at essentially identical $E°$ values (**1** = 0.99 V; **2** = 0.99 V; **3** = 1.00 V vs Ag/AgCl in 0.1 M *n*-$Bu_4N^+PF_6^-$/CH_2Cl_2) that reflect similar energies for the highest occupied molecular orbitals (HOMOs). These values were slightly more anodic than that of unsubstituted quaterthiophene ($E°$ = 0.80 V vs Ag/AgCl), consistent with a slight lowering of the HOMO energy upon introduction of the alkylphenyl end-caps.[28] The electrochemical properties indicated that thin films of **1**−**3** would behave as *p*-channel semiconductors in a TFT configuration. Moreover, the identical $E°$ values suggested a unique opportunity to probe the relationship between crystal structure and electronic transport separate from any contributions from the electronic properties of the molecular constituents alone.

Films of **1**−**3** (ca. 300 Å thick) were deposited by vacuum sublimation (1 × 10^{-6} Torr, substrate temperature during deposition, $T_{substrate}$, was 50−95 °C) on a thermally grown 3 kÅ thick SiO_2 film on highly doped <100>-oriented single-crystal silicon substrates. Atomic force microscopy (AFM) of sample films, acquired in air using the tapping mode, revealed terraced grains ranging in size from ~0.25 to 1 μm (Figure 2). The heights of the steps separating the terraces increased in the order **1** < **2** < **3**, as expected on the basis of the molecular lengths, **1** (27.14 Å) < **2** (31.12 Å) < **3**

(28) Meerholtz, K.; Heinze, J. *Electrochim. Acta* **1996**, *41*, 1839.

(42.55 Å).[29,30] AFM images at the edge of the films revealed several continuous layers suggesting partial layer-by-layer growth (Figure 2D). Thin films of **3** exhibited cracks within its domains if T_{sub} was 90−95 °C and if the substrate was not cooled slowly following deposition. Cracks were presumably a result of strain upon cooling due to the different thermal expansion coefficients of the organic film and the a-SiO_2/Si substrate.[31] Surprisingly, cracks did not appear to have a detrimental effect on the electrical characteristics of resulting devices.

Specular ($\theta-2\theta$) X-ray diffraction (XRD) revealed peaks for each compound at 2θ values assignable to multiple orders of reflection of a highly oriented film (at least two orders of reflection for each film sample). The d-spacings associated with the first-order reflection (d_{001}) for each film increased in the order **1** (28.0 Å) < **2** (29.5 Å) < **3** (37.7 Å) (Figure 3A), comparable with the step heights observed by AFM. The distance between the terminal methyl groups of molecules **1**−**3** (i.e., the end-to-end distance), estimated by assuming phenylalkane substituents with all-trans propyl and hexyl chains, the all-anti structure of quaterthiophene, (Cambridge Structural Database reference code PEWXAQ02[32]), and the accepted value for the van der Waals radius of the terminal methyl group, increases in the order **1** (27.14 Å) < **2** (31.12 Å) < **3** (42.55 Å).[29,30] Thus, the d_{001} values were smaller than the end-to-end lengths for molecules **2** and **3** and nearly identical for molecule **1**. The d_{001} values are consistent with tilt angles of 0 (**1**), 18.6 (**2**), and 27.6° (**3**), assuming adjacent layers did not interdigitate and that the alkyl chains retain the all-trans configuration and the quaterthiophene cores have the all-anti structure. It seems unlikely that the smaller d_{001} values for **2** and **3** are due to syn conformations in the quaterthiophene cores, as this would likely require in-plane lattice parameters that differ from those observed for compound **1**. It is reasonable to suggest, however, that the smaller-than-expected d_{001} spacings in **2** and **3** might reflect interdigitation of adjacent layers, or possibly the existence of gauche conformations in the alkyl chains, which would be expected to afford smaller d-spacings than all-trans chains. The energy of the gauche conformation is ca. 1 kcal/mol higher than that of the anti conformation, and more dominant packing forces are known to prompt the introduction of gauche conformations in alkane substituents.[33] Rocking curves obtained for films of **1**−**3** revealed full width at half-maximums (fwhm) of 0.03−0.05°, signifying exceptionally low mosaicity of the film (i.e., a high degree of parallelism; a fwhm of <0.1° is regarded as a signature of a highly parallel orientation on a flat, highly uniform substrate).

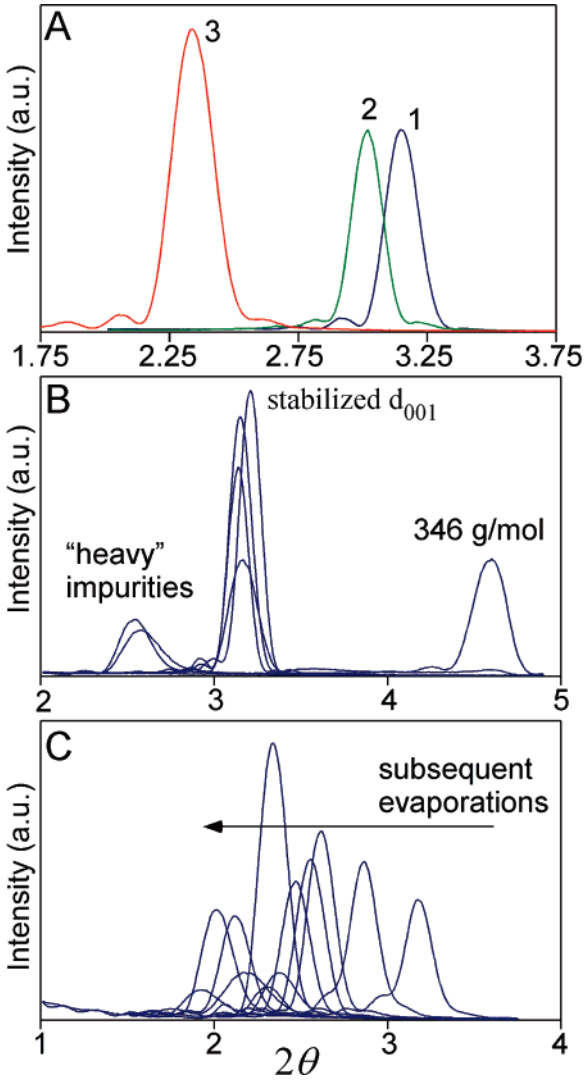

Figure 3. Specular XRD patterns of the (001) reflection (A) for films of **1**−**3**; (B) films of **1** including additional "346" mass observed in mass spectrometry and larger d_{001} spacings after numerous evaporation runs (presumably the interlayer spacing due to films composed of molecules with higher molecular weights than **1**); and (C) films of **3** from numerous evaporation runs illustrating the variation in d_{001} spacing for a given source material.

Films were fabricated of all three compounds from numerous synthesis and evaporation runs. It was observed that the film morphology and d_{001} spacing varied for all three compounds when several evaporation runs were completed sequentially. Compound **1** was found to form crystalline films (grains ≤10 μm in diameter with some sections of the film comprised of wavy, overlapping grains) from initial (1−3) evaporation runs with a freshly synthesized source material. The interlayer spacing of these crystalline films, ($d_{001} \approx 19.0$ Å), was comparable with the previously reported value (18.2 Å).[27] Subsequent evaporations produced films with crystalline grains (~0.25−1 μm) observable by AFM and exhibited a distinctly different d_{001} spacing observable by XRD (28 Å). The d_{001} spacing remained constant for numerous evaporations and then started to shift to larger values (smaller 2θ). This shift in d_{001} to larger values is consistent with impurities

(29) Kuribayashi, M.; Hori, K. *Liq. Cryst.* **1999**, *26*, 809.
(30) Molecular lengths were measured by adding the length of quaterthiophene (C2−C2′ = 14.1 Å), 4.3 Å for each phenyl group (8.6 Å total), 1.45 Å each for the C−C bond from the phenyl to the first carbon in the alkyl chain (2.9 Å total), 1.2 Å for each additional C−C single bond of the alkane chain, and 2 Å for each terminal methyl group (4 Å total).
(31) Coefficients of thermal expansion of crystalline Si, a-SiO_2, and pentacene are 0.249 × 10^{-5}, 0.05 × 10^{-5}, and 1.2−1.3 × 10^{-5}, respectively. (*CRC Handbook of Chemistry and Physics, Internet Version 2005*; Lide, D. R., Ed.; CRC Press: Boca Raton, FL, 2005; http://www.hbcpnetbase.com, and Chapter 6 of this thesis.
(32) Siegrist, T.; Kloc, Ch.; Laudise, R. A.; Katz, H. E.; Haddon, R. C. *Adv. Mater.* **1998**, *10*, 379.
(33) (a) Martin, S. M.; Yonezawa, J.; Horner, M. J.; Macosko, C. W.; Ward, M. D. *Chem. Mater.* **2004**, *16*, 3045. (b) Holman, K. T.; Martin, S. M.; Parker, D. P.; Ward, M. D. *J. Am. Chem. Soc.* **2001**, *123*, 4421.

of higher molecular weight than the material of interest being present in the starting source powder (Figure 3B). Higher-molecular-weight impurities would evaporate after the material of interest had been completely used. A batch of newly synthesized source material was evaluated by mass spectrometry (Finnigan MAT 95, ThermoFinnigan, Waltham, MA), and two masses were observed (346 and 510 g/mol). The 510 mass corresponds to compound **1** and the 346 mass may be attributed to 5,5″-bis(4-methylphenyl)-2,2′-bithiophene, a compound possibly formed by dimerization during synthesis. Therefore, it was determined that the second observed d_{001} spacing (28 Å) was representative of **1** and that films exhibiting this d_{001} spacing were characterized electrically. Sequential evaporations of source material **2** revealed a shift toward larger d_{001} spacings for the first 3 evaporation runs and then the d_{001} spacing stabilized for subsequently deposited films. Source material **3** performed similar to **2**; however, only a few films were observed in a stabilized d_{001} region before the interlayer spacing began to shift to larger values (Figure 3C). For films of compounds **2** and **3**, samples were selected for electrical characterization from the "stabilized" d_{001} region. The observed d_{001} spacing in films of **3** falls between the values reported elsewhere for solution- and vapor-deposited films (37 and 39 Å, respectively).[34]

Thermal analysis was performed to evaluate the presence of impurities. Thermal gravimetric and differential thermal analysis (TG/DTA) were performed using freshly synthesized source material and previously evaporated source material that corresponded to the region of stabilized interlayer spacing. Melting temperatures were observed from the DTA traces obtained in air and were ~220−240 °C for all three compounds. Mass loss was calculated from the TG traces acquired up to 400 °C (presumably below the decomposition temperature for the compounds). A difference in mass loss between freshly synthesized and previously evaporated material was observed. Freshly synthesized source material exhibited mass losses of 10.9, 9.2, and 2.6% for **1**, **2**, and **3** respectively, and previously evaporated material exhibited measured mass losses of 0.2, 6.6, and 0.05%, noticeably lower than the mass loss observed for freshly synthesized material. The change in mass loss after a few evaporation runs indicates that light impurities were present in the freshly synthesized materials. Vapor-phase purification[35] of source materials was attempted; however, materials would either burn or produce too little material for evaporation runs.

One of the factors that influence the transport properties of crystalline organic films in TFTs is their molecular packing (i.e., the crystal structure). The structures of crystalline organic films, particularly ones expected to adopt layered structures, often can be deduced from their bulk crystal structure.[36,37] Structural characterization of **1**−**3**, however, has been frustrated by our inability to obtain crystals of sufficient quality for single-crystal X-ray diffraction. Even if the single-crystal structures (also exhibiting polymorphism)[38−40] were known, the growing evidence for "thin-film" phases[41,63] in organic films with structures different from those of their bulk forms requires independent structural characterization of the thin films.[42−45] This is particularly important because transport in TFTs is thought to occur in the molecular layers near the dielectric layer above the gate electrode.[46] Furthermore, the observation that structures of thin-film phases are influenced by the substrate material[47−56] argues that structural characterization of these films should be performed directly on the dielectric material (typically amorphous SiO_2) of the TFT used for characterization of the transport properties.

Despite the apparent high degree of crystallinity in thin films, XRD patterns of powders of **1**−**3** were characterized by a small number of peaks with low intensities, suggesting poor crystallinity of the bulk materials. Grazing incidence X-ray diffraction (GIXD) was performed on thin films of these materials in order to characterize the in-plane molecular packing, which is crucial to understanding 2D transport. Our laboratory recently reported a preliminary GIXD characterization of a pentacene monolayer (a *p*-channel organic semiconductor) grown on an amorphous *a*-SiO_2 dielectric layer[57] that appears to adopt a crystal structure similar to the so-called thin film phase.[58] A principal advantage of GIXD is the ability to characterize the structure of films grown on the SiO_2 dielectric layer instead of relying on inference from data obtained by techniques that require other substrates, such as electron diffraction.[59−63]

(34) Mushrush, M.; Facchetti, A.; Lefenfield, M.; Katz, H. E.; Marks, T. J. *J. Am. Chem. Soc.* **2003**, *125*, 9414.
(35) Laudise, R. A.; Kloc, C.; Simpkins, P. G.; Siegrist, T. *J. Cryst. Growth* **1998**, *187*, 449.
(36) Ward, M. D. *Chem. Rev.* **2001**, *101*, 1697.
(37) Hooks, D. E.; Fritz, T.; Ward, M. D. *Adv. Mater.* **2001**, *13*, 227.
(38) Antolini, L.; Horowitz, G.; Kouki, F.; Garnier, F. *Adv. Mater.* **1998**, *10*, 382.
(39) Fichou, D. *J. Mater. Chem.* **2000**, *10*, 571.
(40) Facchetti, A.; Yoon, M.-H.; Stern, C. L.; Hutchison, G. R.; Ratner, M. A.; Marks, T. J. *J. Am. Chem. Soc.* **2004**, *126*, 13480.
(41) Ostoja, P.; Maccagnani, P.; Gazzano, M.; Cavallini, M.; Kengne, J. C.; Kshirsagar, R.; Biscarini, F.; Melucci, M.; Zambianchi, M.; Barbarella, G. *Synth. Met.* **2004**, *146*, 243.
(42) Minakata, T.; Imai, H.; Ozaki, M.; Saco, K. *J. Appl. Phys.* **1992**, *72*, 5220.
(43) Jentzsch, T.; Juepner, H. J.; Brzezinka, K.-W.; Lau, A. *Thin Solid Films* **1998**, *315*, 273.
(44) Dimitrakopoulos, C. D.; Brown, A. R.; Pomp, A. *J. Appl. Phys.* **1996**, *80*, 2501.
(45) Bouchoms, I. P. M.; Schoonveld, W. A.; Vrijmoeth, J.; Klapwijk, T. M. *Synth. Met.* **1999**, *104*, 175.
(46) Dodabalapur, A.; Torsi, L.; Katz, H. E. *Science*, **1995**, *268*, 270.
(47) Lang, P.; Ardhaoui, M. El; Wittmann, J. C.; Dallas, J. P.; Horowitz, G.; Lotz, B.; Garnier, F.; Straupe, C. *Synth. Met.* **1997**, *84*, 605.
(48) Lang, P.; Horowitz, G.; Valat, P.; Garnier, F.; Wittmann, J. C.; Lotz, B. *J. Phys. Chem. B* **1997**, *101*, 8204.
(49) Prato, S.; Floreano, L.; Cvetko, D.; Renzi, V. De; Morgante, A.; Modesti, S. *J. Phys. Chem. B* **1999**, *103*, 7788.
(50) Chen, X. L.; Lovinger, A. J.; Bao, Z.; Sapjeta, J. *Chem. Mater.* **2001**, *13*, 1341.
(51) Yoshikawa, G.; Kiguchi, M.; Ikeda, S.; Saiki, K. *Surf. Sci.* **2004**, *559*, 77.
(52) Nagamatsu, S.; Kaneto, K.; Azumi, R.; Matsumoto, M.; Yoshida, Y.; Yase, K. *J. Phys. Chem. B* **2005**, *109*, 9374.
(53) Loi, M. A.; Como, E. Da; Dinelli, F.; Murgia, M.; Zamboni, R.; Biscarini, F.; Muccini, M. *Nat. Mater.* **2005**, *4*, 81.
(54) DeLongchamp, D. M.; Sambasivan, S.; Fischer, D. A.; Lin, E. K.; Chang, P.; Murhpy, A. R.; Fréchet, J. M. J.; Subramanian, V. *Adv. Mater.* **2005**, *17*, 2340.
(55) Heiner, C. E.; Dreyer, J.; Hertel, I. V.; Koch, N.; Ritze, H.-H.; Widdra, W.; Winter, B. *Appl. Phys. Lett.* **2005**, *87*, 093501.
(56) Da Como, E.; Loi, M. A.; Murgia, M.; Zamboni, R.; Muccini, M. *J. Am. Chem. Soc.* **2006**, *128*, 4277.
(57) Fritz, S. E.; Martin, S. M.; Frisbie, C. D.; Ward, M. D.; Toney, M. F. *J. Am. Chem. Soc.* **2004**, *126*, 4084.
(58) Ruiz, R.; Mayer, A. C.; Malliarus, G. G.; Nickel, B.; Scoles, G.; KAzimirov, A.; Kim, H.; Headrick, R. L.; Islam, Z. *Appl. Phys. Lett.* **2004**, *85*, 4926.

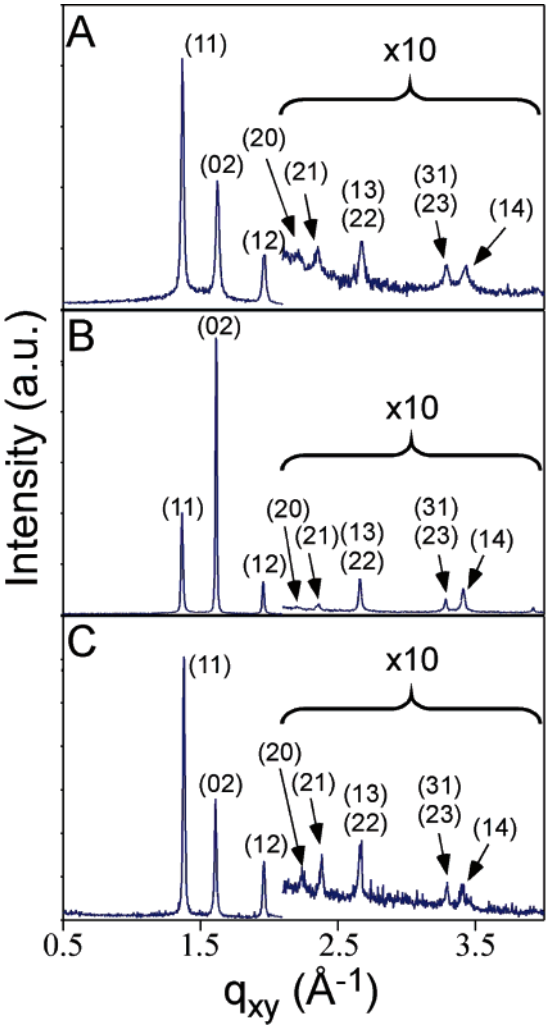

Figure 4. GIXD patterns for 300 Å thick films of **1**−**3** (A−C). Miller indices of peak assignments are labeled.

GIXD data obtained for films of **1**−**3** (ca. 300 Å thick) revealed numerous diffraction peaks consistent with a high degree of in-plane crystalline order (Figure 4). Each diffraction pattern could be indexed to a rectangular in-plane unit cell ($\gamma = 90°$) with dimensions consistent with two molecules per unit cell. In-plane unit-cell areas are nearly identical for **1**−**3** (44.1, 44.4, and 43.8 Å^2, respectively), indicating similar in-plane packing. Table 1 summarizes the calculated lattice parameters, area, interlayer spacing, molecular length, molecular tilt, unit-cell volume, and density. It is possible that compound **3** has a slightly smaller in-plane unit-cell area than **1** and **2**; however, further GIXD experiments would be necessary to verify this.

Electrical Characterization. The transport properties of thin films of **1**−**3** were characterized in a thin film transistor (TFT) configuration with top-contacts. The I_D-V_G characteristics for **1**−**3** (Figure 5) demonstrate that the mobile carriers are holes and that the calculated linear mobilities,

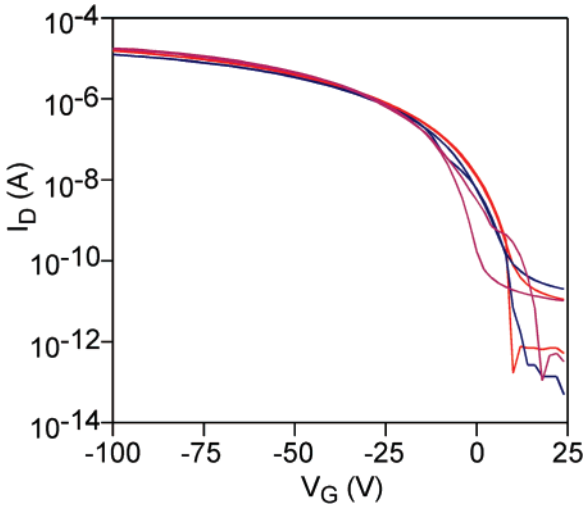

Figure 5. Overlapping transfer curves for materials **1**−**3**. Trace and retrace characteristics are shown for each semiconductor.

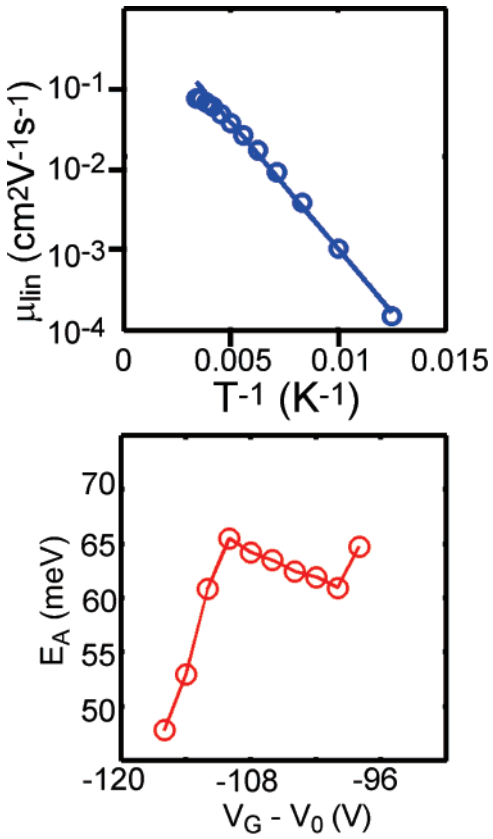

Figure 6. (A) Arrhenius plot of mobility vs temperature and (B) activation energy, E_A, plotted vs $V_G - V_0$ for a TFT with a film of **3**.

$\mu_{lin} \cong 0.05 \pm 0.01$, 0.04 ± 0.01, 0.06 ± 0.01 cm^2/Vs for **1**, **2**, and **3**, respectively, are nearly identical. These values are comparable to those reported previously for **3**[34] and roughly 2 orders of magnitude lower than that of pentacene, a current benchmark for organic TFTs. The I_{on}/I_{off} ratios, however, ranged from 1×10^6 to 1×10^8, which are exceptionally

Table 1. Lattice Parameters, In-Plane Unit-Cell Area, Interlayer Spacing, Molecular Length, Molecular Tilt, Unit-Cell Volume, and Density for Oligothiophenes 1−3

molecule	a (Å)	b (Å)	γ	area (Å^2)	d_{001} (Å)	molecular length (Å)	molecular tilt (deg)	V (Å^3)	D (g/cm^3)
1	5.70	7.74	90°	44.1	28.0 ± 0.1	27.14	0	1235	1.37
2	5.71	7.78	90°	44.4	29.5 ± 0.3	31.12	18.6	1311	1.43
3	5.61	7.81	90°	43.8	37.7 ± 0.6	42.55	27.6	1652	1.31

high for organic TFTs and are much improved in comparison to values reported for **3**.[34] Related molecules without the added phenyl group present in compounds **2** and **3** have been reported to have comparable mobilities but undesirably low I_{on}/I_{off} ratios.[6,64] This implies that the addition of the alkylphenyl groups in **1**−**3** increased the I_{on}/I_{off} ratio. Perhaps this is due to the electron withdrawing character of the alkylphenyl groups which slightly raises the oxidation potential of the thiophene core, making the material somewhat less susceptible to air oxidation and thereby lowering I_{off}, a point noted earlier by Marks and colleagues.[21] It is also interesting that oligothiophenes end-substituted with perfluoroalkylphenyl groups have been shown to exhibit *n*-channel conductivity in TFTs, consistent with further lowering of the HOMO and LUMO levels due to the additional electron withdrawing effects of fluorine.[21]

To evaluate the role of traps in the transport properties of films of **1**−**3**, the electrical characteristics of TFTs were evaluated from 80 to 295K. Mobility of **3** increased with temperature, and an activation energy of 55 meV was extracted from an Arrhenius plot (Figure 6A). It was also instructive to determine the variation in E_A over values of V_G in the linear region (high V_G). A range in E_A of ∼20 meV over 20 V (in V_G) was observed, suggesting a distribution of trap energies (Figure 6B). Films of **2** exhibited hysteresis for temperatures less than 240 °C and films of **1** exhibited hysteresis after being pumped under a vacuum for 24 h, in both cases preventing calculation of an activation energy (for **1** and **2**). Films of **1** were evaluated for bias stress[65] by repeating the electrical measurements using a periodically pulsed V_g.[66] This reduced some of the hysteresis, indicating that some of the trapping was due to bias stress. The remaining hysteresis was removed when the devices were tested in light, indicating that deep traps were present in the film.

Conclusion

Thin films of a series of alkylphenyl-substituted quaterthiophenes displayed reasonable mobilities and exceptional I_{on}/I_{off} ratios, rendering them useful for applications in OTFTs. Structural characterization revealed increasing interlayer spacings consistent with molecular lengths and implying an increase in molecular tilt. In-plane unit-cell areas were nearly identical for **1**−**3**, indicating similar molecular packing. This was corroborated by the nearly identical carrier mobilities measured in TFTs of **1**−**3**. Thermal analysis and XRD of numerous film samples provided insight to impurities and process variability present in the source materials.

Acknowledgment. The authors thank C. R. Newman for writing the Matlab code used to analyze TFT electrical data and extract transport properties and P. V. Pesavento for writing the Matlab code with a pulsed V_g in order to evaluate devices for bias stress. This work was supported primarily by the University of Minnesota Materials Research Science and Engineering Center, under the MRSEC program of the National Science Foundation (Award Number DMR-0212302). A.M.A. was a visiting undergraduate fellow from Hamline University (St. Paul, MN) partially funded by the National Science Foundation Summer Research Program in Solid-State Chemistry (Award DMR-0303450). C. F. Prendergast was a visiting undergraduate fellow from Trinity College (Dublin, Ireland), partially supported by the University of Minnesota MRSEC. GIXD was carried out at the Stanford Synchrotron Radiation Laboratory, a national user facility operated by Stanford University on behalf of the U.S. Department of Energy, Office of Basic Energy Sciences. Mass spectrometry was carried out at the University of Minnesota Department of Chemistry Mass Spectrometry Facility.

CM062831V

(59) Lovinger, A. J.; Davis, D. D.; Dodabalapur, A.; Katz, H. E.; Torsi, L. *Macromolecules* **1996**, *29*, 4952.
(60) Dinelli, F.; Moulin, J.-F.; Loi, M. A.; Como, E. D.; Massi, M.; Murgia, M.; Muccini, M.; Biscarini, F. *J. Phys. Chem. B* **2006**, *110*, 258.
(61) Wu, J. S.; Spence, J. C. H. *J. Appl. Crystallogr.* **2004**, *37*, 78.
(62) Drummy, L. F.; Martin, D. C. *Adv. Mater.* **2005**, *17*, 903.
(63) Mattheus, C. C.; Dros, A. B.; Baas, J.; Oostergetel, G. T.; Meetsma, A.; de Boer, J. L.; Palstra, T. T. M. *Synth. Met.* **2003**, *138*, 475.
(64) Facchetti, A.; Mushrush, M.; Yoon, M.-H.; Hutchison, G. R.; Ratner, M. A.; Marks, T. J. *J. Am. Chem. Soc.* **2004**, *126*, 13859.
(65) Street, R. A.; Salleo, A.; Chabinyc, M. L. *Phys. Rev. B* **2003**, 68, 085316/1.
(66) Lemmi, F.; Street, R. A. *IEEE Trans. Electron. Dev.* **2000**, *47*, 2404.